Polyester artificial ligament modified with a polyphenol-zinc layer for controlled and targeted release of ciprofloxacin

Applied Surface Science 708 (2025) 163712

Contents lists available at ScienceDirect

Applied Surface Science

journal homepage: www.elsevier.com/locate/apsusc

Full Length Article

Polyester artificial ligament modified with a polyphenol-zinc layer for controlled and targeted release of ciprofloxacin

Jakub Reczkowski [a], Martyna Maria Pruszkowska [a], Marcel Jakubowski [a], Maria Ratajczak [b], Łukasz Ławniczak [a], Wojciech Szymkuć [c], Marcin Chodkowski [d], Malgorzata Antos-Bielska [d], Małgorzata Krzyżowska [d], Silvia Spriano [e], Mariusz Sandomierski [a,*]

[a] Institute of Chemical Technology and Engineering, Poznan University of Technology, ul. Berdychowo 4, 60-965 Poznań, Poland
[b] Institute of Building Engineering, Poznan University of Technology, ul. Piotrowo 5, 60-965 Poznań, Poland
[c] Institute of Structural Analysis, Poznan University of Technology, ul. Piotrowo 5, 60-965 Poznań, Poland
[d] Military Institute of Hygiene and Epidemiology, Kozielska 4, 01-163 Warsaw, Poland
[e] DISAT Department, Politecnico di Torino, corso Duca degli Abruzzi 24, 10129 Torino, Italy

ARTICLE INFO

Keywords:
Polyester artificial ligaments
Surface modification
Polyphenol
Ciprofloxacin

ABSTRACT

Tendon and ligament injuries often necessitate surgical intervention with the use of artificial implants due to their complex nature and the difficulties associated with natural tissue regeneration. This study investigates a novel surface modification method for polyester artificial ligaments (PEAL) to enhance their antimicrobial properties and biocompatibility. A polyphenol-zinc layer was synthesized on PEAL using epigallocatechin gallate (EGCG) and zinc cations, which allowed for the adsorption of ciprofloxacin (CIPRO) to achieve prolonged antibacterial activity. Comprehensive analyses, including UV–Vis spectroscopy, scanning electron microscopy (SEM), and X-ray photoelectron spectroscopy (XPS), confirmed the successful synthesis of the layer and the drug adsorption. The modified PEAL exhibited significant improvements in hydrophilicity, antioxidant capacity, and a sustained release of CIPRO over four hours. Antimicrobial tests demonstrated enhanced effectiveness against *Escherichia coli, Pseudomonas aeruginosa,* and *Staphylococcus aureus*, with the highest inhibition rate observed for *E. coli*. Microbiological studies also demonstrated the ability of the modified PEAL to inhibit biofilm formation on their surface. Cytotoxicity studies indicated minimal toxicity for the modified samples, supporting their biocompatibility and potential for biomedical applications. Expression studies of inflammatory markers in two different cell lines showed no negative impact on the cellular inflammatory response. This innovative approach presents a promising solution for reducing infection risks and improving outcomes in the repair of the musculoskeletal system.

1. Introduction

Tendon and ligament damage are among the most common injuries to the musculoskeletal system, alongside muscle tear injuries. The increasing average life expectancy, combined with society's growing interest in physical activity, increases the risk of these injuries. Treatments of tendon and ligament injuries include methods that do not require surgery and act through the biophysical stimulation of damaged tissues – physiotherapy, cryotherapy, or the use of ultrasounds [1]. However, most of these types of injuries require surgeries, sometimes with several revisions to regain full physical fitness. The surgical techniques used include manual repair of damaged tissues, autografts, and allografts [2]. In recent years, the use of functional materials for this type of surgery has become increasingly popular, as they are designed to ensure high mechanical strength of the reconstructed tendons or ligaments.

However, it is important to match and adapt the materials used to the microenvironment of the damaged tendon or ligament [3]. Non-degradable polymers have found considerable application in this area, and are used to produce artificial tendons and ligaments due to their biochemical stability and good mechanical strength [4]. Apart from proper healing and restoration of full fitness, a significant problem in the treatment of this type of injury is also the risk of bacterial adhesion to the implants and the development of biofilm, which may lead to

* Corresponding author.
E-mail address: mariusz.sandomierski@put.poznan.pl (M. Sandomierski).

https://doi.org/10.1016/j.apsusc.2025.163712
Received 6 March 2025; Received in revised form 26 May 2025; Accepted 1 June 2025
Available online 2 June 2025

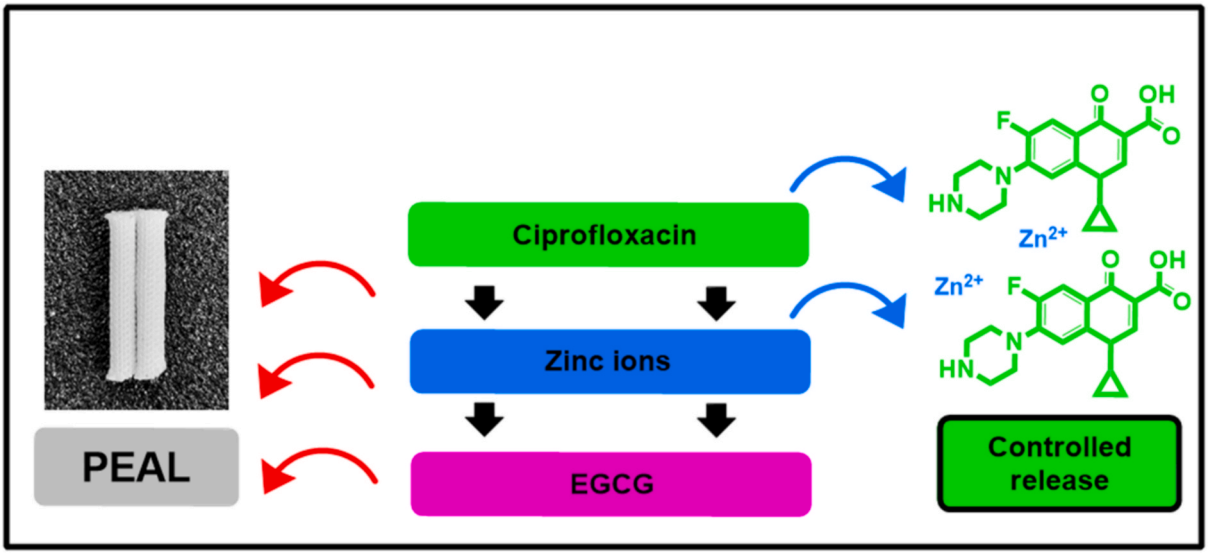

Fig. 1. Scheme of conducted modification.

pharmacologically difficult-to-treat infections [5]. A local antibacterial and/or antibiofilm action by the implant surface is a key strategy to reduce the risk of infection of artificial tendons or ligaments and to avoid the discomfort and costs of revision surgery. Polymer materials intended for artificial tendons and ligaments have already been modified to improve their antibacterial properties, but the limited number of reports indicate that this subject is still poorly understood. A tentative was made by using polydopamine layers with an admixture of silver ions, or by applying complex polymer films of natural and synthetic origin [6,7]. New modifications of artificial tendons and ligaments with multifunctional action are needed for higher efficacy.

One promising way for surface modification of polyester artificial ligaments (PEAL) uses polyphenols. Polyphenols are secondary metabolites produced by plants, playing a key role in defense mechanisms, highly effective in facing oxidative stress and inflammation through their antioxidant properties. Epigallocatechin gallate (EGCG) stands out among polyphenols for its significant biological properties. Due to its antioxidant properties, it is a component of many dietary supplements, and may also have an impact on the treatment of obesity-related conditions or cardiovascular diseases, due to the control of oxidative stress [8]. EGCG can also be used as an active anticancer substance because it inhibits topoisomerases responsible for DNA replication [9]. However, the poor solubility, bioavailability and stability make this compound poorly effective through systemic and dietary assumptions which is why local action through surface modification of an implant is a promising strategy. EGCG can form coatings through oxidative autopolymerization, but partial oxidation turns into a loss of antioxidant properties [10]. Numerous hydroxyl groups in the chemical structure of EGCG enable the formation of coordination bonds with bivalent or trivalent metal cations (e.g., Cu^{2+}, Ca^{2+}, Zn^{2+}, Al^{3+}) [11]. This chemical bond can be exploited as an alternative for EGCG's surface grafting. Additionally, EGCG and zinc cations can synergize their antioxidant and antibacterial properties [12]. EGCG does not show cytotoxicity if maintained in a proper concentration limit and, due to its anti-cancer properties, it is a preventive strategy in reducing the risk of recurrence at a site where cancer has been removed [13]. However, the integration of EGCG with a complementary antibacterial agent is necessary for targeting different bacterial functions and achieving effective prevention.

Ciprofloxacin (CIPRO) is an active substance used in the treatment of numerous bacterial infections. It belongs to the group of fluoroquinolone antibiotics, and it is usually administered orally. Its chemical structure opens up the possibility of forming coordination bonds due to the presence of carbonyl and hydroxyl groups in close proximity. CIPRO can form complex bonds with various metal cations such as copper, nickel, cobalt, and zinc [14]. Moreover, the complex of zinc cations and this active substance revealed the highest antimicrobial activity.

Oral administration of CIPRO also has some drawbacks, such as fast elimination from the human body and several side effects on the digestive system [15].

Finding an appropriate way to administer this antibiotic can increase its effectiveness and minimize harmful and severe effects on the human body. The local release of this antibiotic has already been tested by modifying the surface of e.g. titanium implants to prevent peri-implantation infections [16].

Therefore, in this work, PEAL samples were covered by a layer of EGCG doped with zinc cations. The created layer was capable of attaching CIPRO molecules on its surface. This modification opened a way to improve the antimicrobial properties of PEAL, which is crucial to achieve successful treatment of tendon/ligament injuries. To the best of our knowledge, such a modification has never been performed before. The CIPRO adsorption and release profiles were investigated by UV–Vis spectroscopy. Coated PEAL was investigated using scanning electron microscopy (SEM) and X-ray photoelectron spectroscopy (XPS) techniques. Additionally, the breaking force of the obtained materials was tested to determine whether the applied modification affects the mechanical properties of the material. The antimicrobial activity and cytotoxicity were also studied. The diagram and the idea of the modification carried out are shown in Fig. 1.

2. Methods and materials

2.1. Materials

PEAL samples (Tricomed, Poland) made of polyester were used to conduct the experimental part. The reagents used to synthesize the polyphenol layer: EGCG (purity – 99.5 %), ammonium persulfate (purity – 98.0 %), and zinc acetate dihydrate (purity – 99.5 %) were purchased from Merck and Sigma Aldrich. The active substances tested – CIPRO (purity 99.5 %), 2,2-Diphenyl-1-picrylhydrazyl (DPPH) (purity – 99.0 %), and L-ascorbic acid (purity – 99.5 %) were all purchased from Sigma Aldrich. The compounds used for the simulated body fluid in the release studies were also purchased from Sigma Aldrich. The reagents used for the studies were used without further purification.

2.2. Preparation of the polyphenol-zinc layer

PEAL samples were cut into smaller parts of 1 cm in length. The polyphenol-zinc solution was prepared by dissolving 50 mg of EGCG and 2.39 mg of zinc acetate hydrate in TRIS-HCL buffer (10 mM, pH = 8.5). After all ingredients were solubilized, 24.88 mg of ammonium persulfate was added to the solution and stirred to complete dissolution. PEAL samples were immersed in the prepared solution and placed in a hydrothermal reactor for 24 h at 70 °C. Samples after that stage of modification were named PEAL-EGCG-Zn^{2+}. After preparing the polyphenol-zinc layer on PEAL samples, they were dried for 24 h at 36.6 °C.

2.3. Drug adsorption – ciprofloxacin (CIPRO)

The adsorption of CIPRO was studied by placing both unmodified and surface-modified samples of PEAL in Eppendorf tubes and flooding them with a solution of this active substance. The samples were flooded with 1 ml of CIPRO solution (0.02 mg of CIPRO dissolved in 1 ml of distilled water). Eppendorf tubes were placed on an orbital shaker (150 rpm), and drug adsorption on the surface of samples was checked after every 24 h using UV–VIS spectroscopy. The total adsorption time of CIPRO on the modified surface was 72 h. The resulting materials were named PEAL-EGCG-Zn^{2+}CIPRO. The amount of retained drug was determined based on six repetitions.

2.4. Ciprofloxacin (CIPRO) release

The modified PEAL samples were placed in Eppendorf tubes. They were flooded with 1 ml of SBF solution and placed on a temperature-controlled orbital shaker (200 rpm), set at 37 °C. The tested solution was collected from Eppendorf tubes into cuvettes and examined using a UV–VIS spectrophotometer, where the amount of drug released was measured after each hour of the examination. The exact composition of the SBF solution (per 1000 ml) contained 8.035 g of NaCl; 0.355 g of $NaHCO_3$; 0.225 g of KCl; 0.231 g of $K_2HPO_4{\cdot}3H_2O$; 0.072 g of Na_2SO_4; 0.6112 g of TRIS and 0–5 ml of HCl [17].

2.5. Methods

2.5.1. UV–VIS spectroscopy

To study the amount of CIPRO adsorbed on both unmodified and modified surfaces of PEAL samples during the adsorption process, measurements were conducted in the range of 250–450 nm (λ max = 272 nm), with the final value calculated as the mean of six replicates. Determination of the amount of released active substance was also performed in that range, with the result expressed as the mean of three measurements. The examination was determined by a UV–VIS spectrophotometer UV-2600 (Shimadzu, Japan). To analyze the studied amount of CIPRO, a calibration curve in water and SBF solution was prepared for adsorption and drug release analysis.

2.5.2. Inductively coupled plasma – mass spectrometry

To determine the weight assay of zinc doped into the created polyphenol layer, ICP-MS analysis was conducted. PEAL samples of determined mass after the stage of forming a polyphenol-zinc layer were dissolved in a mineralizer in aqua regia (12 ml). After mineralization and cooling, it was quantitatively transferred to a 25 ml flask and made up to the mark with water. A 4-point standard curve was prepared, and the zinc assay in ppb was determined on its basis and then converted to weight %.

2.5.3. Molecular modelling

Molecular modelling was employed in order to investigate the coordination of zinc cations in a system which includes both EGCG and CIPRO molecules. The calculations were carried out using the density function theory (DFT) and the B3LYP/3-21G basis set using the Gaussian 09 software. Each structure was prepared as a separate model using the graphical interface of the HyperChem 8.0 software. After initial geometrical optimization and inspection of each structure, the separate models were combined in order to investigate the interaction energy and geometrical parameters following the coordination of Zn^{2+} by both EGCG and CIPRO.

2.5.4. Scanning electron microscopy (SEM)

To determine a microscopic analysis of the modified surface of PEAL samples, a scanning electron microscope VEGA 3 (TESCAN) was used. Photos were taken after each step of the performed modification, and the results are shown at hundredfold and four hundredfold times magnification.

2.5.5. X-ray photoelectron spectroscopy (XPS)

PEAL samples were conducted to X-ray photoelectron spectroscopy. XPS analysis was performed using a PHI VersaProbeII Scanning XPS system equipped with monochromatic Al Kα (1486.6 eV) X-rays focused into a 100 μm spot, scanning across an area of 400 μm × 400 μm. The photoelectron take-off angle was 45°, and the analyzer's pass energy was set to 117.50 eV (0.5 eV step size) for survey scans and 46.95 eV (0.1 eV step size) for high-resolution spectra targeting the C 1s, O 1s, N 1s, and F 1s regions. A dual-beam charge neutralization system, employing 7 eV Ar^+ ions and 1 eV electrons, ensured stable surface potential regardless of sample conductivity. All spectra were calibrated to the unfunctionalized, saturated C–C carbon C 1s peak at 285.0 eV. The analytical chamber operated at pressures below 3.0×10^{-9} mbar. Spectral deconvolution was conducted using PHI MultiPak software (v.9.9.3), with the Shirley method applied for background subtraction.

2.5.6. Water contact angle (WCA)

To study the hydrophilic properties of both unmodified and modified PEAL samples, they were tested by measuring the water contact angle. The WCA was measured using a Theta Lite Optical Tensiometer. Samples were placed on a leveled table, and image capture was initiated using specialized software. A drop of distilled water was applied to each sample, and the process was recorded for 30 s. The first image in which the droplet had fully stabilized on the sample was selected for analysis. The contact angle was then calculated using the appropriate software (Attention theta). Three types of samples were evaluated, and the results represent the average measurements for each sample type, based on the mean of four samples per type.

2.5.7. Antioxidant assay by DPPH measurement

The DPPH test was used to evaluate the antioxidant capacity of the prepared materials. The study was conducted following protocols available in the literature [18]. For this purpose, a DPPH solution in anhydrous ethanol with a final absorbance of 0.509 was first prepared. Then, the prepared samples (1 cm in length) were placed in 1 mL of the prepared solution for 30 min in the absence of light. After this time, their absorbance was measured at a wavelength of 517 nm, with the results expressed as the mean of three replicates. A pure DPPH solution was used as a control. The amount of DPPH (in %) was calculated using the following formula:

$$Antioxidant\ \ activity = \left(\frac{A517c - A517s}{A517c}\right)*100\% \quad (1)$$

where: A517c represents the absorbance of the control sample at a wavelength of 517 nm, and A517s represents the absorbance of the tested sample at a wavelength of 517 nm.

To compare the antioxidant capacity of the obtained material, the ability to neutralize prepared DPPH by an L-ascorbic acid solution, a natural antioxidant, was also investigated. For this purpose, a stock solution of L-ascorbic acid with an initial concentration of 250 μM was prepared. Serial dilutions were then made to achieve concentrations

down to approximately 3.9 μM. To 1 mL of the DPPH solution, 0.1 mL of the ascorbic acid solution was added, and the mixture was kept in the dark for 30 min. After this time, the samples were analyzed using UV–VIS spectroscopy, and the antioxidant capacity was determined using Equation (1).

2.5.8. Breaking load

To determine the breaking load of PEAL samples before and after modification, a universal testing machine Instron Electropuls E1000 (Instron) was used. The primary goal of this study was to determine if the proposed modifications influence the breaking force. Before tests, samples were conditioned at least 48 h at (20 ± 1) °C and (50 ± 5) % relative humidity. Ligament ends were looped around circular elements secured in the grips. The test was displacement-controlled with a constant machine crosshead speed of 30 mm/min. Each result is an average of three tests.

2.5.9. Antibacterial activity – Inhibition zone

The antibacterial activity was assessed using *Staphylococcus aureus* ATCC 25923, *Escherichia coli* ATCC 25922, and *Pseudomonas aeruginosa* ATCC 27853 using the disc diffusion method. A total of 100 μL of bacterial suspension with a turbidity equivalent to 0.5 on the McFarland scale was evenly spread on Mueller-Hinton agar (MHA) plates. Each PEAL sample was cut into 0.5 cm pieces, and one piece was placed on the surface of the inoculated agar plate. The negative control consisted of Mueller-Hinton broth (MHB) alone. All samples were incubated at 37 °C for 24 h. Antibacterial activity was determined by measuring the diameter of the inhibition zone formed around the sample. The

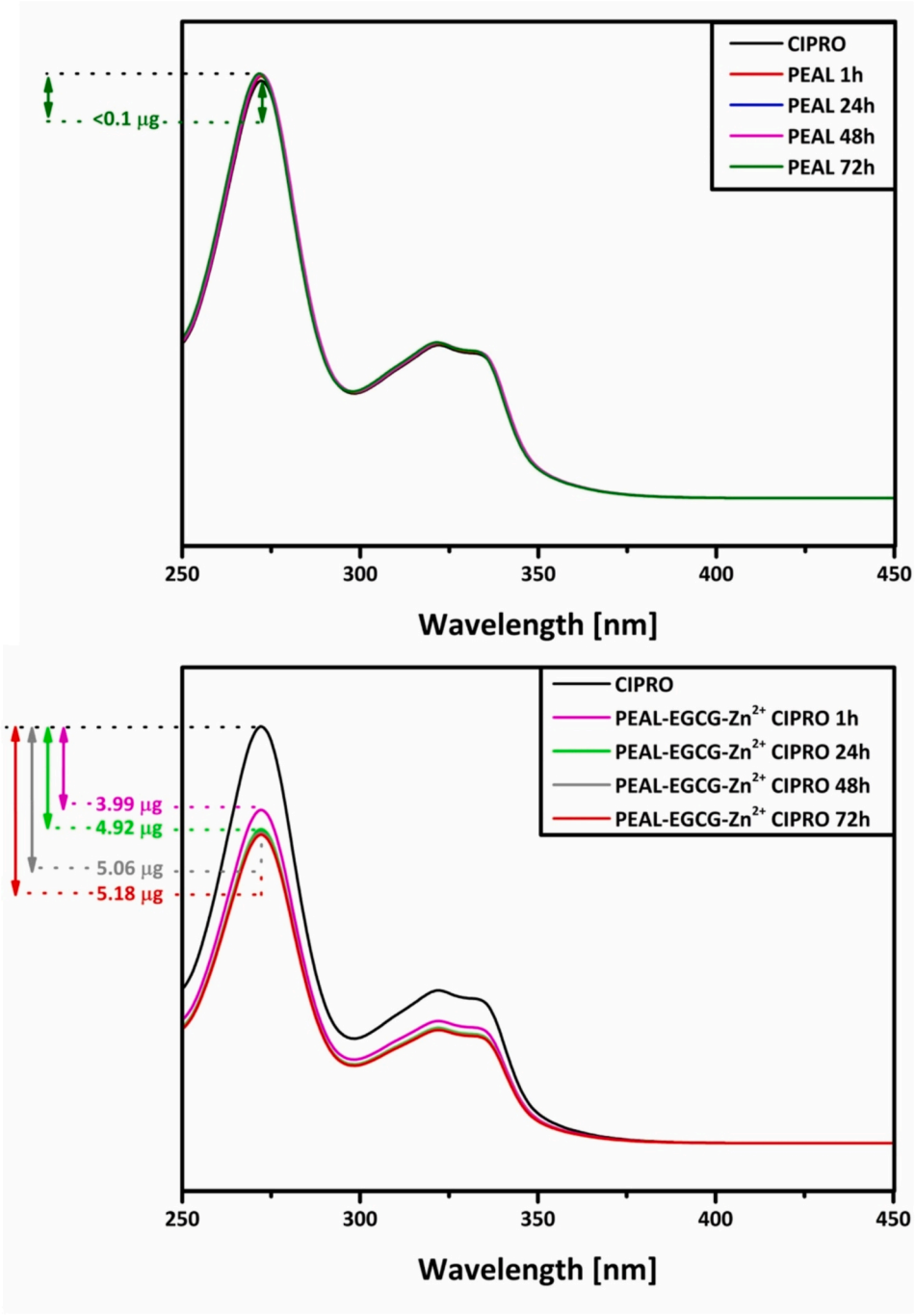

Fig. 2. CIPRO adsorption on the unmodified and modified surfaces of PEAL samples.

inhibition zones were measured in millimeters (mm), with the PEAL diameter (5 mm) subtracted from the total inhibition zone.

2.5.10. Evaluation of bacterial biofilm formation on ligament surfaces

To assess the ability of the tested ligament materials to support bacterial biofilm formation, two complementary methods were employed. Biofilm was allowed to form on the surface of ligament fragments incubated with a bacterial suspension under controlled conditions. Quantification of the biofilm was performed using crystal violet staining, which measures total biofilm biomass, and the MTT assay, which evaluates the metabolic activity of the adherent bacterial cells. Both methods provided insight into the extent and viability of the biofilm formed on each ligament variant.

2.5.11. Quantification of biofilm biomass – Crystal violet staining

Following incubation, the bacterial suspension was carefully removed from each well, and the ligament samples were gently rinsed three times with phosphate-buffered saline (PBS) to remove non-adherent cells. The samples were then transferred to fresh wells and fixed by adding 500 μL of 0.3 % formalin, followed by a 10-minute incubation at room temperature. After fixation, the samples were washed again with PBS and stained with 500 μL of 0.1 % crystal violet for 15 min. Excess dye was removed by thorough rinsing, and the samples were air-dried for 15 min. To solubilize the bound dye, 500 μL of 95 % ethanol was added to each well and incubated for 20 min. Subsequently, 100 μL of the extracted solution was transferred to a 96-well plate, and absorbance was measured at 595 nm using a Omega Microplate Spectrophotometer (BioTek Instruments, Inc., Winooski, VT, USA).

2.5.12. Assessment of metabolic activity of biofilm – MTT assay

To evaluate the metabolic activity of biofilm formed on the ligament surfaces, the MTT assay was performed. After incubation, the bacterial suspension was removed from each well, and the ligament samples were gently rinsed three times with phosphate-buffered saline (PBS) to eliminate non-adherent cells. The samples were then transferred to fresh wells, and 500 μL of MTT solution (0.075 % MTT in PBS) was added to each well. After 2 h of incubation at 37 °C, the MTT solution was carefully removed, and the samples were gently rinsed with PBS.

Subsequently, the ligaments were transferred to new wells, and 375 μL of dimethyl sulfoxide (DMSO) and 125 μL of glycine buffer (0.1 M, pH 10.2) were added to solubilize the formazan crystals. After 15 min of incubation, 100 μL of the resulting solution was transferred to a 96-well plate, and absorbance was measured at 570 nm using a microplate reader.

2.5.13. Cell viability

The effect of PEAL samples on cell viability was assessed using the MTT assay. Human keratinocyte (HaCaT), adenocarcinomic human alveolar basal epithelial (A549), and African green monkey kidney (Vero) cells were suspended and seeded in 96-well plates at a density of 5×10^3 cells per well in 200 μl of medium and incubated overnight. Cells were then incubated with PEAL samples for 24 h. A solution of3-(4,5-dimethylthiazol-2-yl)-2,5-diphenyltetrazolium bromide (MTT; Sigma-Aldrich) was prepared by dissolving it in PBS at 5 mg/ml, and 100 μl of this solution was added to each well. An additional 100 μl of culture medium was added to reach a final concentration of 2.5 mg/ml, and the plates were incubated for one hour. Dimethyl sulfoxide (DMSO; Sigma-Aldrich, MA) was used to dissolve the resulting formazan crystals. The quantity of the colored formazan derivative was measured by recording the absorbance at 570 nm using an Omega Microplate Spectrophotometer (BioTek Instruments, Inc., Winooski, VT, USA). Cell viability was expressed as the percentage of viable cells relative to the untreated control. All experiments were performed in triplicate.

2.5.14. Gene expression analysis of inflammatory Cytokines

To evaluate the inflammatory response induced by the tested materials, A549 and HaCaT cells were cultured in Dulbecco's Modified Eagle Medium (DMEM) supplemented with 10 % fetal bovine serum and 1 % penicillin–streptomycin under standard conditions (37 °C, 5 % CO_2). After reaching approximately 80–90 % confluence, cells were exposed for 24 h to PEAL, PEAL-EGCG-Zn^{2+}, and PEAL-EGCG-Zn^{2+}CIPRO. Total RNA was isolated using the MagnifiQ™ 1 Total RNA Plus instant kit (A&A Biotechnology, Poland) according to the manufacturer's instructions. The experiment was conducted in three independent replicates. Isolated RNA was reverse transcribed into complementary DNA (cDNA) using GoScript™ Reverse Transcriptase (Promega, USA). Quantitative PCR (qPCR) was performed using GoTaq® Probe qPCR Master Mix (Promega, USA) with specific primers and probes for IL-6, IL-10, IL-1β, and IFN-β. The housekeeping gene GAPDH served as an internal reference for normalization. All reactions were run in technical triplicates. Relative gene expression levels were calculated using the $2^{-\Delta\Delta Ct}$ method. Data were analyzed using standard qPCR software and presented as mean ± standard deviation. Statistical significance between groups was evaluated using one-way ANOVA followed by appropriate post hoc tests, with $p < 0.05$ considered significant.

2.5.15. Statistical analysis

All numerical data were expressed as mean ± standard deviation (SD). Statistical comparisons between multiple groups were performed using one-way analysis of variance (ANOVA), followed by Tukey's multiple comparisons test to identify statistically significant differences. A p-value of less than 0.05 was considered statistically significant. Each experimental group included at least three independent replicates. Graphical data were visualized as bar charts with appropriate statistical annotations. All analyses were performed using GraphPad Prism (version 10.4.2, GraphPad Software, San Diego, CA, USA).

3. Results

During the initial phase of the research, a study was undertaken to synthesize the polyphenol-zinc layer on the polyester material and the eventual adsorption of CIPRO. This analysis was performed with a UV–Vis spectroscope, and the results are presented in Fig. 2. The first graph clearly shows that unmodified PEAL is unable to adsorb CIPRO on its surface. A significant change in the surface properties of this material can be seen from the second diagram. The results show that the polyphenol-zinc layer on the surface of PEAL created the possibility of the adsorption of CIPRO. This is due to an EGCG layer with zinc cations in its structure [19]. It is worth emphasizing that zinc ions are attached to the polyphenol layer through coordination interactions with phenolic –OH groups. Zinc ions in the prepared layer serve as active sites for drug adsorption, also utilizing coordination interactions [20]. It is also worth adding that π-π interactions may occur between the drug and the layer, stabilizing the drug's coordination on the surface. The quantity of the active substance adsorbed onto the surface of the modified PEAL gradually increases over time, as demonstrated by successive measurements. The adsorption process concluded after 72 h, with the modified PEAL sample retaining a maximum of 5.18 μg (±0.42 μg) of CIPRO, corresponding to 26 % of the total amount of CIPRO initially present in the prepared solution. The samples used in our study were 1 cm long. However, the artificial ligaments used during surgery are significantly longer. Therefore, the amount of loaded drug will be much higher, and the amount of 5.18 μg of ciprofloxacin adsorbed on the surface of a 1 cm long ligament is sufficient.

The next step of examining the obtained material was to define the weight assay of zinc adsorbed on the surface of the created polyphenol-zinc layer. The sample named PEAL-EGCG-Zn^{2+} contains about 5 μg of zinc, which corresponds to 0.076 μmol per 1 cm length. This confirms the presence of these ions on the surface after the first stage of PEAL modification. Zinc cations are the key factor that enables the adsorption of an active substance. This is confirmed by the amount of CIPRO

Table 1
Energy values calculated for the studied models.

Energy of individual components [Hf]	
EGCG	−1667.38
CIPRO	−1142.08
Zn^{2+}	−1769.74
total	−4579.21
Energy of the EGCG-Zn^{2+}CIPRO system [Hf]	
	−4579.96
Energy of interaction [Hf]	
	−0.75

adsorbed on the surface of the modified PEAL, which is 5.18 μg, corresponding to 0.016 μmol. As can be observed, the number of moles of adsorbed ciprofloxacin is smaller than the number of moles of zinc ions. This can be explained by the fact that, for example, some zinc ions may be unavailable to CIPRO due to steric hindrances or due to prior strong coordination with the catechol groups of EGCG within the layer. Additionally, there is a possibility that the CIPRO molecule may interact with more than one Zn^{2+} ion due to the presence of various functional groups in its structure [21].

The results of molecular modelling confirmed that zinc cations are readily coordinated by both EGCG and CIPRO, which results in the stabilization of the system (as indicated by the lower energy of the system compared to the total energy of individual components presented in Table 1). The interaction of all components resulted in a notable decrease of energy for the studied system (by approx. 475 kcal/mol). Zinc cation was coordinated by two oxygen atoms originating from hydroxyl groups in EGCG and two oxygen atoms which formed the carbonyl and carboxyl group in CIPRO. The general geometry of the coordinated system resembled that of the hybridisation of a sp3 carbon, with distances between Zn^{2+} and the corresponding ranging from 1.84 to 1.91 Å (Fig. 3, the oxygen atoms of CIPRO are in the same plane as the central Zn cation, whereas the oxygen atoms of EGCG are behind and in front of the plane, respectively).

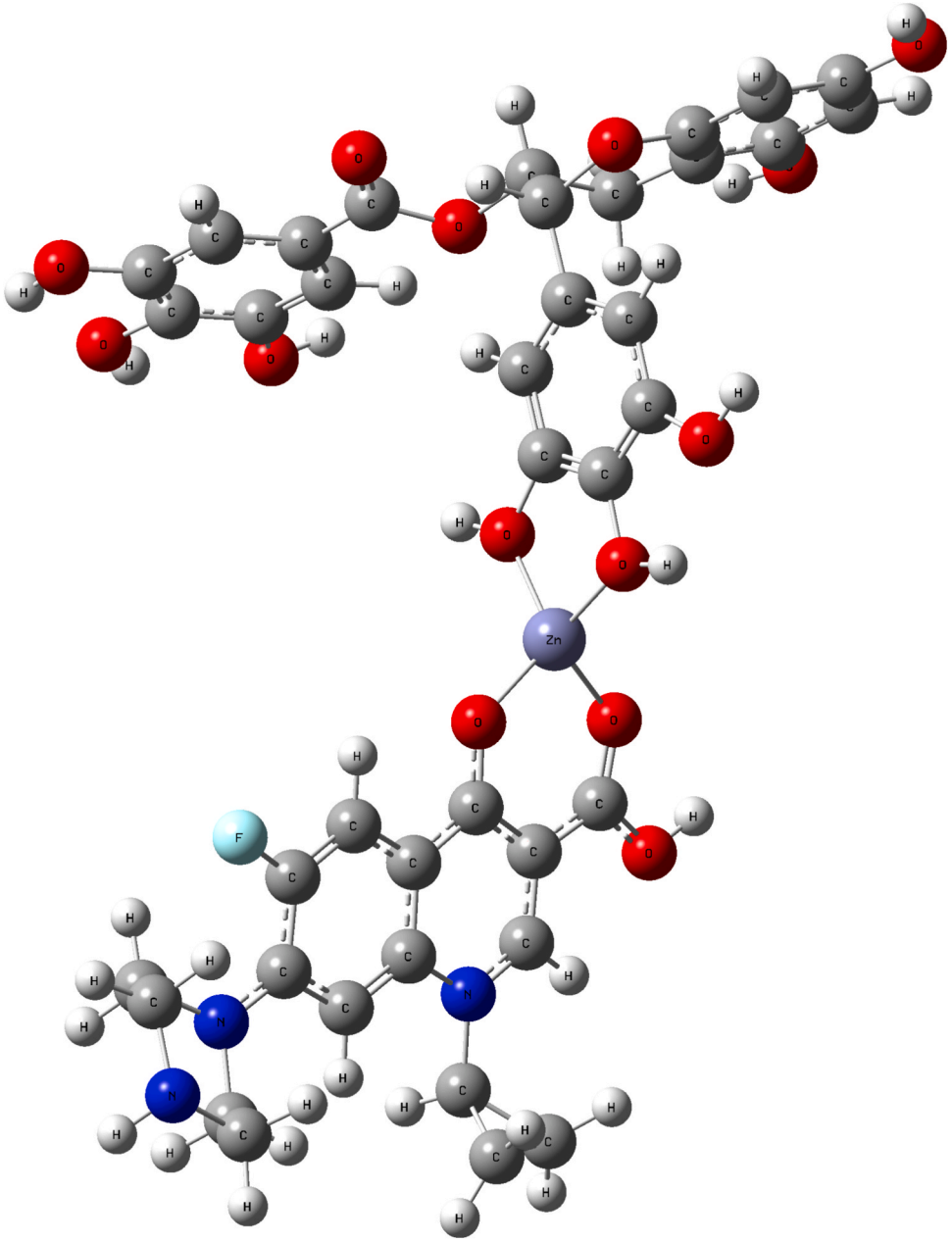

Fig. 3. Graphical representation of the EGCG-Zn^{2+}CIPRO coordination model.

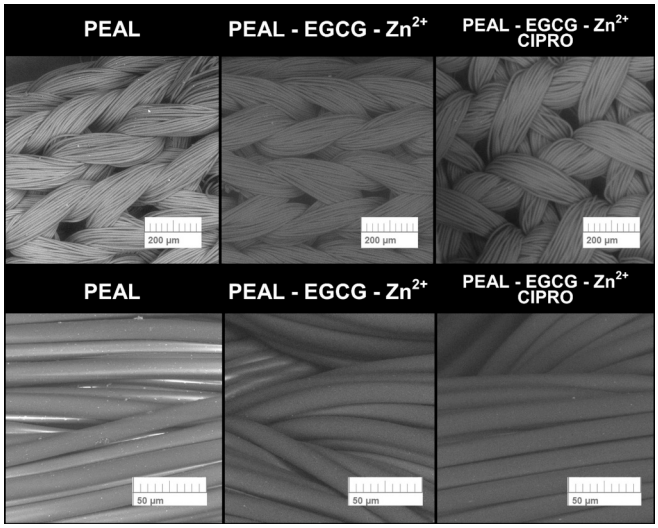

Fig. 4. SEM images of the tested PEAL at each modification stage, captured at 100x and 400x magnifications.

Table 2
Surface concentrations of chemical bonds derived from the analysis of XPS data for all examined samples.

	C				N	
Binding energy [eV]	284.6	286.2	288.6	291.3	399.6	401.1
Compounds/Bonds	C=C	C–C C-O C-N	O-C=O	shake-up	C-NH	NH_4^+
PEAL	45.4	15.4	12.0	0.7	0.0	0.0
PEAL-EGCG-Zn^{2+}	44.1	18.7	9.8	0.6	0.0	0.0
PEAL-EGCG-Zn^{2+} CIPRO	41.5	22.1	9.1	0.6	1.0	0.7
	O				**F**	
	531.7 O=C		533.2 O-C		687.0 F^-	
PEAL	11.7		14.8		0.0	
PEAL-EGCG-Zn^{2+}	10.7		16.1		0.0	
PEAL-EGCG-Zn^{2+}CIPRO	10.0		14.6		0.4	

The next analysis focused on defining the impact of the performed modification on the morphology of the analyzed material. PEAL samples at each modification stage were taken for SEM analysis. The obtained results are presented in Fig. 4. There are no clear differences between the analyzed samples. Additionally, the performed modification did not cause any damage to the macrostructure of PEAL. This is crucial because creating a polyphenol-zinc layer on the surface of the analyzed material does not impact the structural properties of PEAL samples.

The obtained materials were also taken to XPS analysis to check the presence of the created polyphenol-zinc layer on the surface of modified PEAL samples.

The results are presented in Table 2 and in Figs. 5 and 6.

The C 1s spectra for all analyzed samples were fitted with four lines typical for polyesters: the first line at 284.6 eV indicating C=C type sp^2 aromatic rings, second line at 286.2 eV points out the existence of C–C sp^3 type carbon and/or C-O and/or C-N bonds, next line at 288.6 eV comes from the O-C=O type bonds, and the last one at 291.3 eV indicate shake-up structure presence which is attributed to aromatic rings [22]. The shake-up excitation originates from the sp^2 carbon and its aromatic forms and is an additional parameter confirming the presence of this type of bond. The O 1s spectra were fitted with two lines, with the first line centered at 531.7 eV indicating O=C type bonds and the second line at 533.2 eV, which indicates the presence of O-C bonds [20,21]. The F1s spectra were fitted with one line centered at 687.0 eV, pointing out the existence of fluoride in the sample [23]. Spectrum collected in N 1s region was fitted with two lines first centered at 399.6 eV attributed to C-N bonds and/or –NH– [22] and second line at 401.1 eV originating either from NH^{4+} compounds or C=N groups [24,25]. A significant increase in the share of single C-O bonds for the samples at each modification stage indicates the successful synthesis of the polyphenolic layer. One can also notice a decrease in the share of characteristic bonds that make up the tested polyester, i.e., C=C and O-C=O bonds. This is due to the fact that the synthesized polyphenol layer covers the tested material, and mainly the bonds building the polyphenol layer are visible. Another important result from the XPS analysis is that in the PEAL-EGCG-Zn^{2+}CIPRO sample, bonds with nitrogen and fluorine are present. These elements occur only in CIPRO's structure, proving the effectiveness of adsorption on the surface of the tested PEAL.

Another characterization technique was the water contact angle at each modification phase. These measurements, shown in Fig. 7A, reveal that the contact angle values for the modified samples are significantly lower than those of the unmodified sample surface (P value < 0.0001). This indicates that the modified surfaces are hydrophilic, while bare PEAL samples were hydrophobic. Moreover, values of contact angle equal to zero were recorded after 30 s of measurement for the modified samples, which means they are super-hydrophilic. It is an important feature for applying PEAL in the human body because it is well-known that chemical affinity between body fluids and surface implants results in a positive outcome. After all, the first step of tissue integration is the adsorption of ions and biomolecules from body fluids. Additionally, the hydrophilic nature of the prepared material suggests enhanced cytocompatibility because several cells adhere only on surfaces with a surface energy lower than 30–40 mN/m, which means a water contact angle lower than 65° [26].

To further characterize the material, an antioxidant capacity test was also conducted. The results of this study are shown in Fig. 7B. The unmodified PEAL samples exhibited minimal ability to react with the model free radical used in this study, DPPH. After modifying PEAL with a polyphenol layer, this capacity increased significantly (up to 31.5 ± 3.30 %, P value < 0.0001). The primary mechanism of free radical neutralization by the adsorbed layer is their reaction with phenolic groups (–OH) present in the EGCG structure [27]. After drug adsorption, the ability to react with DPPH decreased slightly (to 27.96 ± 1.97 %), but this change is not statistically significant. This reduction may be attributed to steric hindrance, as CIPRO molecules were present on the surface of the material, which hinders the radical's access to the surface. Due to the retained ability to react with DPPH after drug adsorption, it can be assumed that the layer will exhibit some degree of anti-inflammatory activity. Additionally, to facilitate the assessment of antioxidant capacity, we conducted comparative studies using ascorbic acid. The results are shown in Fig. 7C. As can be observed, a similar amount of DPPH neutralized by a single ligament sample was also neutralized by an ascorbic acid solution in the concentration range of 31.25–62.5 μM.

More specifically, one sample of the artificial ligament was able to neutralize the same amount of DPPH as 0.1 mL of an L-ascorbic acid solution with a concentration of approximately 43 μM.

Another stage of our studies was focused on the specification of the release profile of CIPRO from the modified surface of PEAL. The acquired materials were analyzed to determine the quantity of active substance released and the duration over which this release occurs. Fig. 8 illustrates the CIPRO release profile from the surface of the modified samples. The desorption process took place for 4 h. A prolonged release of CIPRO is crucial to face the risk of infection by microorganisms. A full release of the active substance at the first moment of contact with body fluids would be inappropriate because late infections could occur. The PEAL sample could be alternatively modified by simply sprinkling the surface with antibiotic solutions, but this approach would not generate prolonged antibacterial protection. The quantity of the drug released from PEAL-EGCG-Zn^{2+} is 6.43 μg, equating

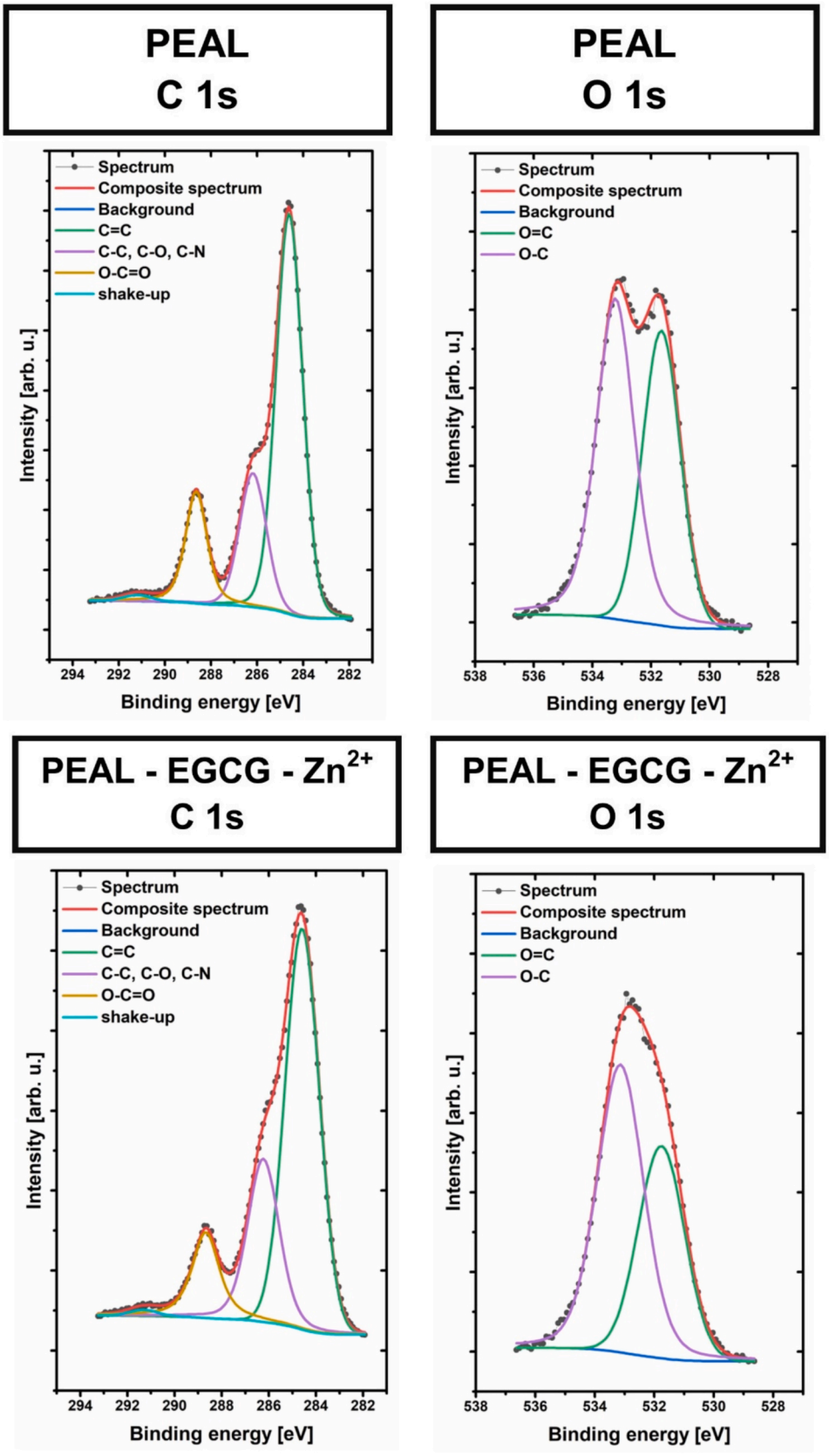

Fig. 5. High-resolution spectra of the modified surface of PEAL samples before drug adsorption.

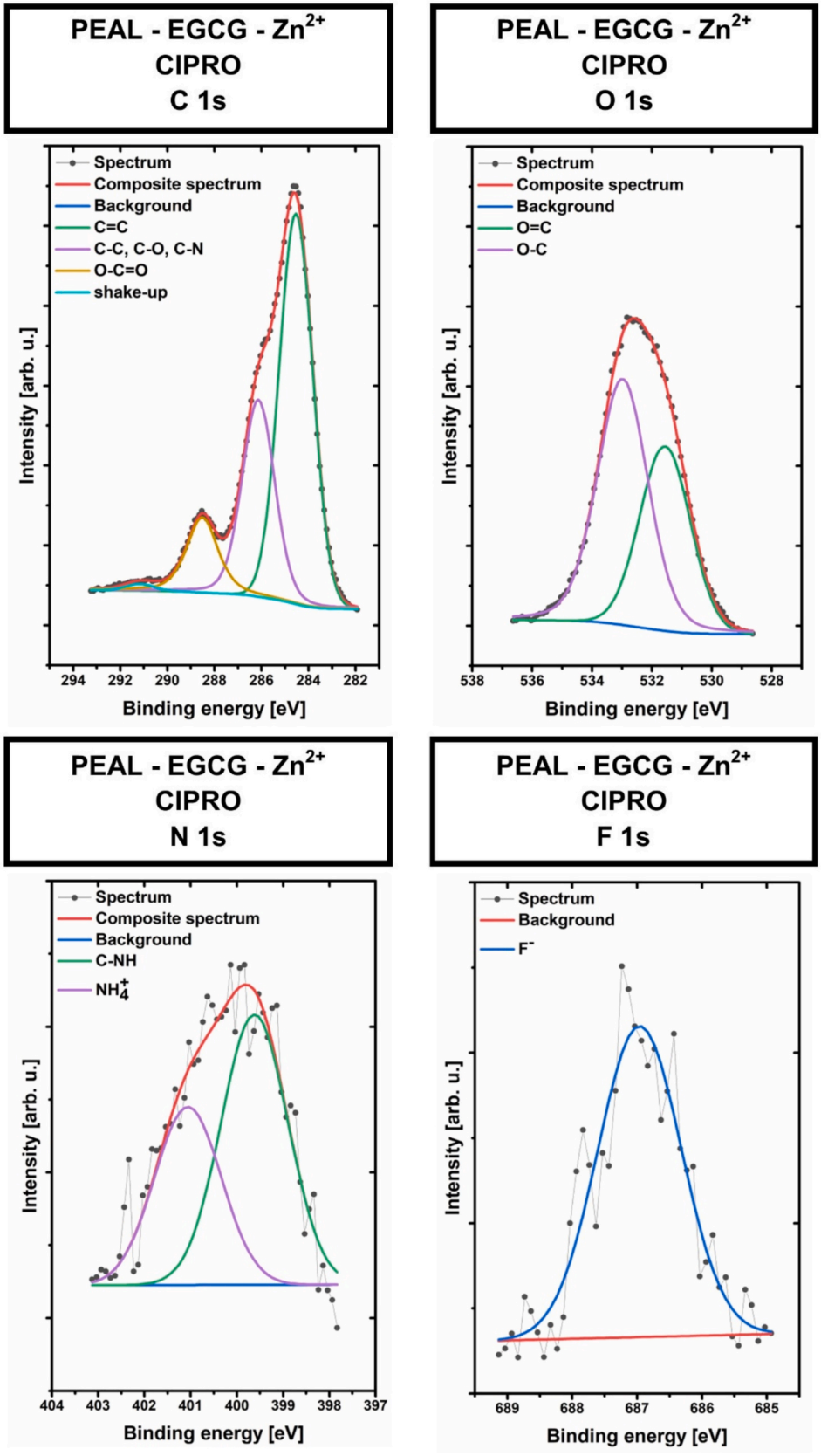

Fig. 6. High-resolution spectra of the modified surface of PEAL samples after drug adsorption.

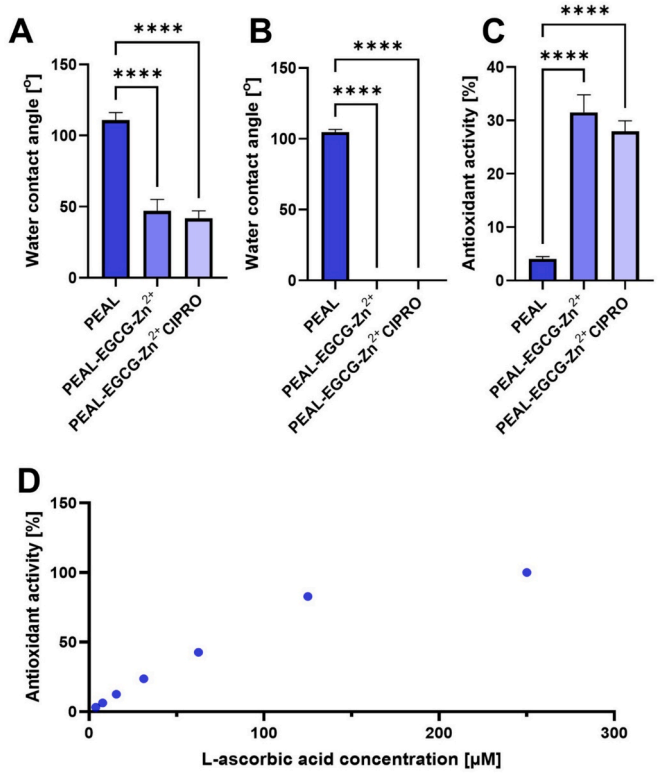

Fig. 7. (A) The water contact angle values after 1s, (B) The water contact angle values after 30 s, (C) The antioxidant activity values of studied ligament samples, (D) The antioxidant activity values for different concentrations of L-ascorbic acid solutions. Results are expressed as mean ± SD (n = 4 for contact angle, and n = 3 for DPPH). Statistical analysis was performed using one-way ANOVA followed by Tukey's multiple comparisons test, with a significance level set at 0.05. Statistically significant differences are indicated by: ****p < 0.0001. Comparisons with p ≥ 0.05 are not marked on the graph.

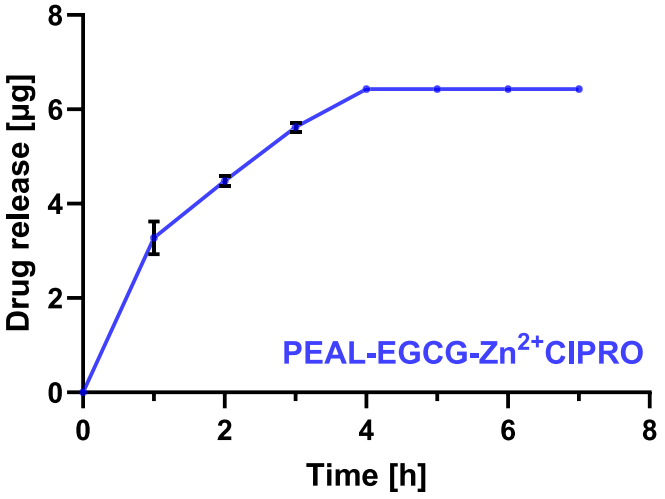

Fig. 8. Release profile of CIPRO from the modified surface of PEAL.

to approximately 124 % of the amount initially adsorbed onto the surface of the modified PEAL. As can be seen, the amount of drug released from PEAL exceeds the amount of drug adsorbed on the surface, as determined by UV–VIS spectroscopy. This may be due to the small number of ciprofloxacin molecules bound to the surface of PEAL through physical interactions.

An important aspect during modification is that the material retains its mechanical properties. This is because its primary function is to replace tissues and bear mechanical loads. For this reason, the tensile strength of the materials described in this work was determined. Mechanical tests revealed that the breaking force was similar for all three investigated ligaments. An average breaking force (± SD) was found to be (395 ± 25) N for PEAL, (400 ± 34) N for PEAL-EGCG-Zn^{2+}, and (402 ± 15) N for PEAL-EGCG-Zn^{2+}CIPRO. The results show that the proposed surface modification method did not influence the ligament breaking force.

Table 3
The inhibition zone of the tested PEAL samples.

	PEAL(I)		PEAL-EGCG − Zn^{2+} (II)		PEAL-EGCG − Zn^{2+} CIPRO(III)
E. coli ATCC 25922	R	R	R	R	39 ± 1
P. aeruginosa ATCC 27853	R	R	R	R	15
S. aureus ATCC 25923	R	R	R	R	14

To examine the antibacterial activity of the unmodified sample and the ones after each stage of modification, they were tested against *Escherichia coli* ATCC 25922, *Pseudomonas aeruginosa* ATCC 27853, and *Staphylococcus aureus* ATCC 25923 using the disc diffusion method. These bacterial strains were selected because they are often associated with bacterial infections at postoperative sites. Additionally, they form biofilms on various surfaces [28,29]. Data in Table 3 are presented as the mean inhibition zone (mm) ± standard deviation (SD) from three independent experiments performed in triplicate, where "R" indicates bacterial resistance, where no measurable inhibition zone was observed.

The results, summarized in Table 3, demonstrate that PEAL and PEAL-EGCG-Zn^{2+} alone exhibited no measurable inhibition zones, indicating resistance (R) to all tested bacterial strains. The lack of an inhibition zone for the sample modified with the polyphenol layer and zinc ions is not surprising, as the antibacterial activity of EGCG is difficult to detect using this test. However, the addition of CIPRO to the PEAL-EGCG-Zn^{2+} sample significantly improved antibacterial efficacy, as shown by inhibition zones of 39 ± 1 mm for E. coli, 15 mm for P. aeruginosa, and 14 mm for S. aureus. These findings confirm the strong antibacterial effect of CIPRO against both Gram-negative and Gram-positive bacteria. Moreover, the result for the *E. coli* strain is almost twice as much as the results for *P. aeruginosa* and *S. aureus*. It confirms that CIPRO is especially effective against *E. coli* strain because of the specific mechanism of action against this Gram-negative bacteria [30]. A positive finding is the ability of the materials to inhibit the growth of *P. aeruginosa* bacteria, as numerous reports indicate that this strain causes infections that are among the most difficult to treat [31]. The obtained results also confirm the broad-spectrum activity of CIPRO [32]. Photos of the registered inhibition zone for the PEAL-EGCG-Zn^{2+}CIPRO sample are presented in Fig. 9A.

In addition to inhibition zone tests, biofilm formation inhibition assays on the PEAL surface were also conducted. For this purpose, bacterial strains of *Staphylococcus aureus* and *Pseudomonas aeruginosa* were selected to represent Gram-positive and Gram-negative groups, respectively. The results are presented in Fig. 9.

As can be shown, the ability of *Pseudomonas aeruginosa* to form biofilm on PEAL, PEAL-EGCG-Zn^{2+}, and PEAL-EGCG-Zn^{2+}CIPRO surfaces was firstly evaluated by crystal violet staining at 1, 4, and 7 days (Fig. 9B). At the 24-hour time point, biofilm biomass on PEAL was significantly higher than on PEAL-EGCG-Zn^{2+}CIPRO ($p < 0.05$), indicating early inhibition of biofilm formation by the antibiotic-modified material. At day 4, a statistically significant reduction in biomass was also observed for the PEAL-EGCG-Zn^{2+}CIPRO surface compared to both PEAL and PEAL-EGCG-Zn^{2+} ($p < 0.05$), suggesting a continued antibiofilm effect. By day 7, the difference between groups narrowed, but PEAL-EGCG-Zn^{2+}CIPRO still exhibited significantly lower biofilm accumulation than PEAL ($p < 0.05$). No statistically significant

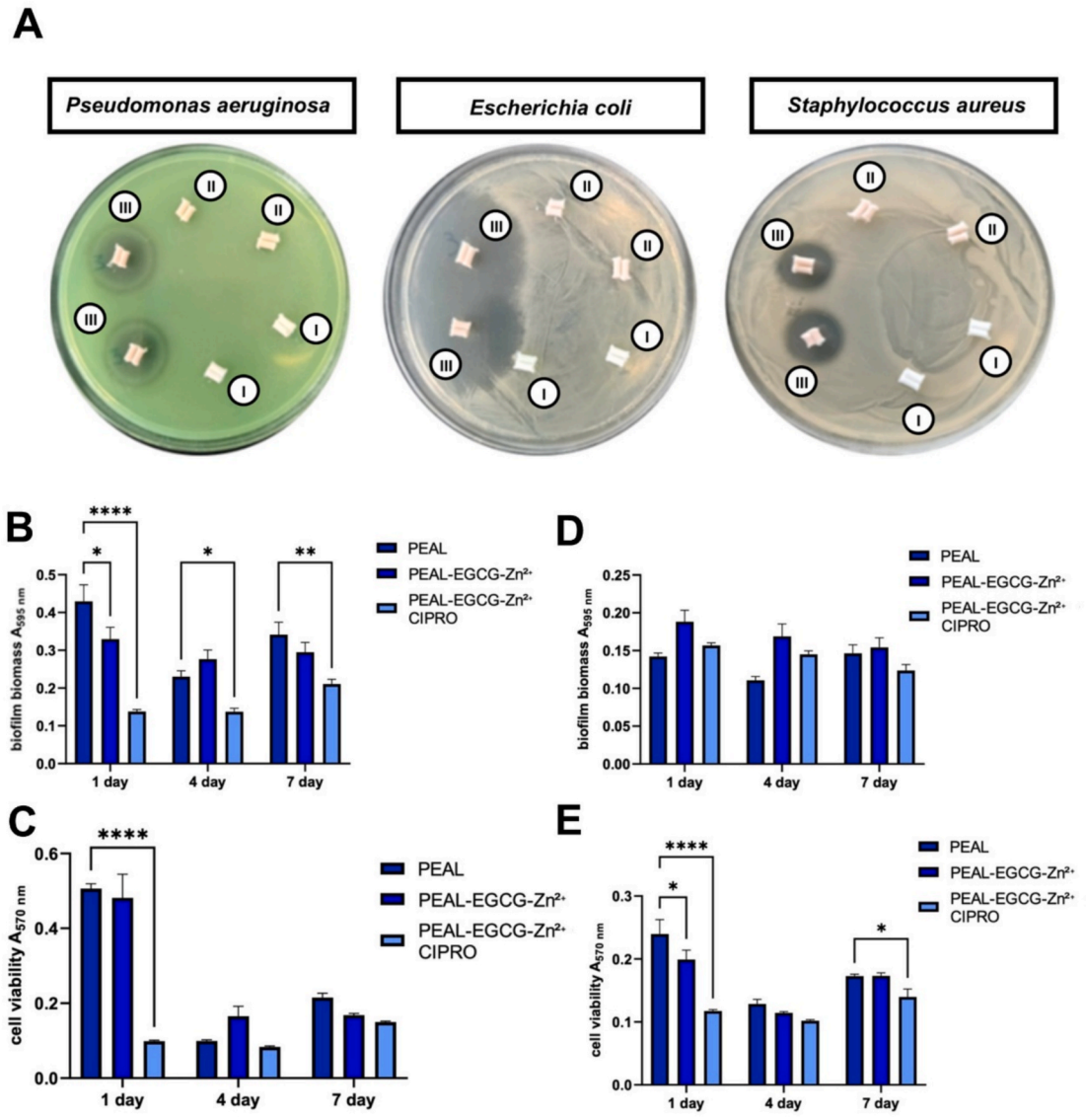

Fig. 9. A) Inhibition zone for each examined strain of the modified PEAL sample B) Biofilm biomass of *Pseudomonas aeruginosa* formed on PEAL-based ligament materials after 24 h, 4 days, and 7 days, C) Metabolic activity of *Pseudomonas aeruginosa* biofilms on PEAL-based ligament materials after 1, 4, and 7 days, D) Biofilm biomass of *Staphylococcus aureus* formed on PEAL-based ligament materials after 1, 4, and 7 days E) Metabolic activity of *Staphylococcus aureus* biofilms on PEAL-based ligament materials after 1, 4, and 7 days. Results are expressed as mean ± SD (n = 3). Statistical tests were performed using PEAL as a reference. Statistical analysis was performed using two-way ANOVA followed by Dunnett's multiple comparisons test, with a significance level set at 0.05. Statistically significant differences are indicated by: *$p < 0.05$, **$p < 0.01$, ***$p < 0.001$, ****$p < 0.0001$. Comparisons with $p \geq 0.05$ are not marked on the graph.

differences were found between PEAL and PEAL-EGCG-Zn^{2+} at any time point, indicating that EGCG and Zn^{2+} were insufficient to suppress biomass development under these conditions. These findings support the role of ciprofloxacin incorporation in effectively limiting *P. aeruginosa* biofilm formation over time. In addition to the crystal violet assay, the MTT assay was also performed to assess the metabolic activity of the bacteria (Fig. 9C). The results exhibited a similar trend to those obtained using the crystal violet assay. A statistically significant reduction in metabolic activity was observed for the PEAL-EGCG-Zn^{2+}CIPRO surface compared to PEAL at the 24-hour time point ($p < 0.005$). This inhibitory effect persisted over time, with the CIPRO-modified surface continuing to demonstrate significantly lower metabolic activity on days 4 and 7 ($p < 0.05$), indicating sustained suppression of bacterial viability. In contrast, no significant differences were observed between PEAL and PEAL-EGCG-Zn^{2+} at any time point, suggesting that the addition of EGCG and Zn^{2+} did not markedly affect *P. aeruginosa* metabolic activity under these conditions.

Similar tests were performed for *Staphylococcus aureus* strain. The crystal violet test (Fig. 9D) showed that after 1, 4, and 7 days, all materials supported similar levels of biomass formation. Overall, no pronounced inhibition of *S. aureus* biofilm biomass was observed for any material. Different results were obtained using the MTT assay. After 1 day, biofilms on PEAL exhibited the highest metabolic activity, with slightly lower activity observed for PEAL-EGCG-Zn^{2+}, and the lowest for PEAL-EGCG-Zn^{2+}CIPRO, indicating an early trend toward reduced bacterial viability on the antibiotic-modified surface. At day 4, metabolic activity was comparable across all groups, with minimal variation. By day 7, biofilms on PEAL and PEAL-EGCG-Zn^{2+} maintained higher metabolic activity than those on PEAL-EGCG-Zn^{2+}CIPRO, although the differences remained moderate. Overall, the data suggest that PEAL-EGCG-Zn^{2+}CIPRO may exert a mild inhibitory effect on *S. aureus* metabolic activity, particularly at the early and late stages of biofilm development.

Infections caused by bacteria growing as biofilms are much more

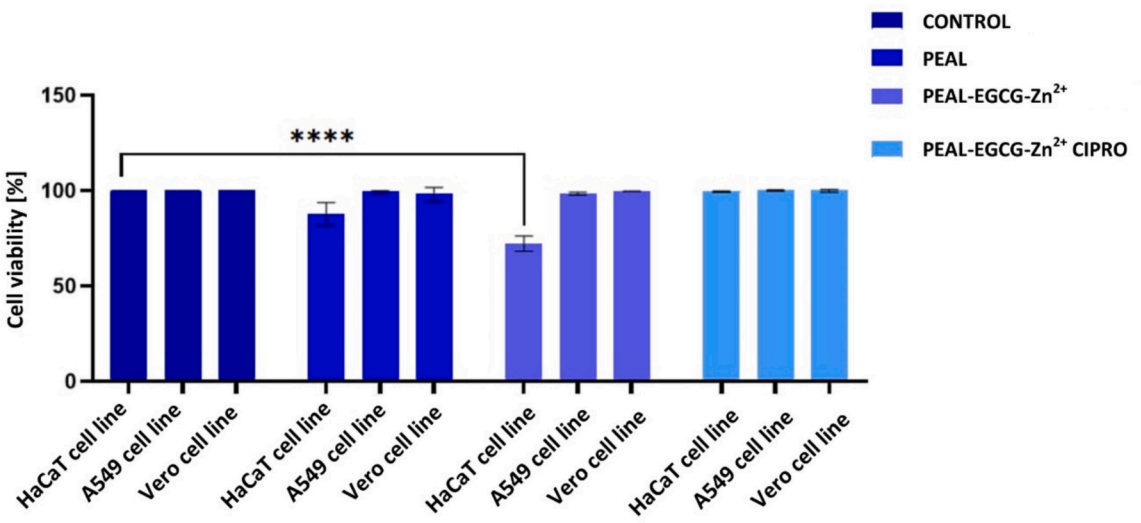

Fig. 10. Cell viability of HaCaT, A549, and Vero cell lines after exposure to PEAL samples. Results are expressed as mean ± SD (n = 3). Statistical tests were performed using PEAL as a reference. Statistical analysis was performed using two-way ANOVA followed by Dunnett's multiple comparisons test, with a significance level set at 0.05. Statistically significant differences are indicated by: *p < 0.05, **p < 0.01, ***p < 0.001, ****p < 0.0001. Comparisons with p ≥ 0.05 are not marked on the graph.

difficult to treat than those caused by free-floating (planktonic) bacteria. As demonstrated by the conducted experiments, the final PEAL-EGCG-Zn^{2+}CIPRO material is capable of inhibiting biofilm formation by both *S. aureus* and *P. aeruginosa*. However, a pronounced antibacterial effect was observed only against *P. aeruginosa*. As previously mentioned, *P. aeruginosa* is regarded as one of the most difficult Gram-negative pathogens to treat, which makes the enhanced activity of the material against this strain particularly promising [31]. These findings are generally consistent with the literature. In a recent study, the authors demonstrated that surfaces modified with polyphenol-based coatings containing metal ions exhibited significantly greater antibiofilm activity against *P. aeruginosa* than against *S. aureus* [33]. Additionally, the lower activity against *S. aureus* may be due to the fact that ciprofloxacin has a stronger effect against *P. aeruginosa* than *S. aureus*. The minimum inhibitory concentration (MIC) values are 0.12–0.25 mg/L for *P. aeruginosa* (ATCC 28753) and 0.25–0.5 mg/L for *S. aureus* (ATCC 29213), respectively [34].

At the final stage of research, the cell viability after exposure to PEAL samples was examined. The cytotoxicity of the investigated materials was evaluated using the MTT assay on HaCaT, A549, and Vero cell lines, and the results are presented in Fig. 10, where the bars represent the percentage of viable cells relative to the control group.

The results show that the modified sample before the adsorption of CIPRO named PEAL-EGCG-Zn^{2+} significantly reduced cell viability compared to the control group ($p < 0.0001$), indicating a cytotoxic effect on HaCat cell lines. In contrast, the control unmodified PEAL and PEAL-EGCG-Zn^{2+}CIPRO exhibited minimal cytotoxicity, with cell viability exceeding 90 % across all cell types. It is a crucial feature of the proposed modification of PEAL presented in this work. Proved non-cytotoxicity makes the PEAL modified with a polyphenol-zinc layer safe to apply in the human body. Moreover, the results of this analysis claim the biocompatibility of the proposed way of changing the surface of the material used in the reconstruction of ruptured ligaments. The non-toxicity of the modified PEAL also ensures the possibility of long-term use, which is important in the case of artificial elements of the musculoskeletal system, which are not replaceable over time, and their implantation is a one-time procedure.

Additionally, to gain more insight into the effects of the obtained biomaterials on cells, an analysis of inflammatory marker expression was performed. The study was conducted on A549 and HaCaT cell lines and the results are shown in Fig. 11. In A549 cells, exposure to the

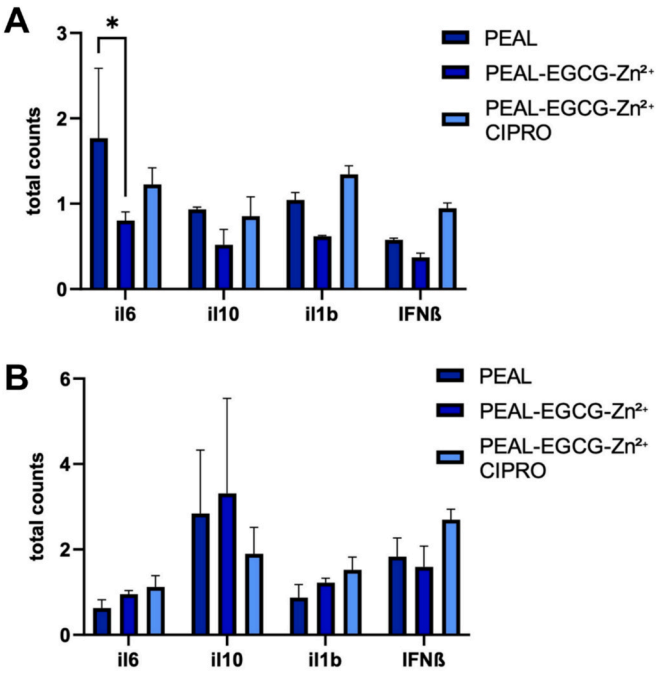

Fig. 11. A) Relative mRNA expression levels of IL-6, IL-10, IL-1β, and IFN-β in A549 cells after 24-hour exposure to synthetic ligament materials, B) Relative mRNA expression levels of IL-6, IL-10, IL-1β, and IFN-β in HaCaT cells after 24-hour exposure to synthetic ligament materials. Results are expressed as mean ± SD (n = 3). Statistical tests were performed using PEAL as a reference. Statistical analysis was performed using two-way ANOVA followed by Dunnett's multiple comparisons test, with a significance level set at 0.05. Statistically significant differences are indicated by: *p < 0.05, **p < 0.01, ***p < 0.001, ****p < 0.0001. Comparisons with p ≥ 0.05 are not marked on the graph.

synthetic ligament materials PEAL, PEAL-EGCG-Zn^{2+}, and PEAL-EGCG-Zn^{2+}CIPRO resulted in only minor changes in the expression of selected cytokine genes when compared to the untreated control. A modest increase in IL-6 (pro-inflammatory cytokine) expression was observed across all materials, with the highest level noted after exposure to PEAL-EGCG-Zn^{2+}CIPRO. IL-1β (pro-inflammatory cytokine) expression was

slightly elevated in all experimental groups, particularly in the PEAL-EGCG-Zn^{2+} condition. IL-10 (anti-inflammatory cytokine) levels showed a subtle upregulation in cells treated with PEAL-EGCG-Zn^{2+}CIPRO, while IFN-β (modulation of the inflammatory response) expression was marginally increased in the presence of both PEAL-EGCG-Zn^{2+} and its combination with CIPRO. In HaCaT keratinocytes, exposure to PEAL, PEAL-EGCG-Zn^{2+}, and PEAL-EGCG-Zn^{2+}CIPRO led to moderate increases in cytokine gene expression relative to the untreated control. Notably, IL-10 expression was elevated in all experimental groups, with the highest level detected in cells treated with PEAL-EGCG-Zn^{2+}. IL-1β showed a marked increase in expression after exposure to PEAL-EGCG-Zn^{2+}, followed closely by PEAL, while the combination with CIPRO resulted in slightly lower expression. As for IFN-β, a modest increase was observed, most prominently in the PEAL-EGCG-Zn^{2+}CIPRO group.

In general, both cell lines in this work showed completely different results in the expression of inflammation markers. Both Zn^{2+} ions and Ciprofloxacin can induce the formation of reactive oxygen species (ROS) with a pro-inflammatory action [35,36]. In the case of A549 cells (a human cell line derived from an alveolar lung carcinoma), studies show that small amounts of Zn^{2+} ions can increase proliferation [37]. Therefore, a decrease in the expression of inflammation markers in the PEAL-EGCG-Zn^{2+} samples is expected. On the other hand, ciprofloxacin, besides its antibacterial action, also exhibits anticancer effects against the A549 cell line [38]. This causes an increase in the expression of inflammation markers, especially IL-1 beta and IL-6, in the PEAL-EGCG-Zn^{2+}CIPRO samples. In the case of HaCaT cells, a decreased cell viability was previously observed after incubation with the PEAL and PEAL-EGCG-Zn^{2+} samples. For this reason, an increase in the expression of markers such as IL-6 and IL-10 is not surprising. Some studies also show that HaCaT cells are sensitive to ROS-induced stress [39]. Overall, the conducted studies show that surface modification of PEAL does not significantly negatively affect the expression of inflammation markers. Some of these markers have even lower levels compared to unmodified PEAL. For this reason, the obtained material can be considered cytocompatible.

4. Conclusions

In conclusion, the presented study demonstrated a novel and effective method for enhancing the antimicrobial properties and biocompatibility of polyester artificial ligaments (PEAL) by creating a polyphenol-zinc layer capable of adsorbing CIPRO. The modification successfully improved the surface properties of PEAL, including increased hydrophilicity, antioxidant capacity, and prolonged drug release, while maintaining structural integrity and non-cytotoxicity. Analysis of inflammatory markers showed that the obtained layer does not negatively affect the induction of inflammation in cells. Mechanical tests also showed that the modification does not affect the breaking force of the material. The samples with adsorbed ciprofloxacin on their surface exhibited strong antibacterial activity against all tested bacterial strains, both Gram-positive and Gram-negative, with a particularly strong effect against the *E. coli* strain. Additionally, the antibiotic-modified PEAL membranes were able to inhibit biofilm formation on their surface. These promising findings underscore the potential of the proposed modification in preventing post-implantation infections and promoting better outcomes for ligament repair. Further research and clinical evaluation are recommended to explore this innovative material's long-term efficacy and safety for biomedical applications.

CRediT authorship contribution statement

Jakub Reczkowski: Writing – original draft, Visualization, Methodology, Investigation, Conceptualization. **Martyna Maria Pruszkowska:** Investigation. **Marcel Jakubowski:** Writing – original draft, Investigation. **Maria Ratajczak:** Investigation. **Łukasz Ławniczak:** Investigation, Methodology. **Wojciech Szymkuć:** Investigation, Methodology. **Marcin Chodkowski:** Writing – original draft, Visualization, Methodology, Investigation. **Malgorzata Antos-Bielska:** Writing – review & editing, Methodology, Investigation. **Małgorzata Krzyżowska:** Writing – review & editing, Methodology, Investigation. **Silvia Spriano:** Writing – review & editing, Writing – original draft, Supervision. **Mariusz Sandomierski:** Writing – review & editing, Writing – original draft, Visualization, Supervision, Resources, Project administration, Methodology, Investigation, Conceptualization.

Declaration of competing interest

The authors declare that they have no known competing financial interests or personal relationships that could have appeared to influence the work reported in this paper.

Acknowledgments

This work was produced with financial support from the National Science Centre, Poland (grant no. 2023/51/D/ST5/00144).

This research was funded in whole or in part by National Science Centre, Poland (grant no. 2023/51/D/ST5/00144). For the purpose of Open Access, the author has applied a CC-BY public copyright licence to any Author Accepted Manuscript (AAM) version arising from this submission.

Data availability

Data supporting the findings of this study are available in the open RepOD repository with the identifier https://doi.org/10.18150/O5HXLZ.

References

[1] N.L. Leong, J.L. Kator, T.L. Clemens, A. James, M. Enamoto-Iwamoto, J. Jiang, Tendon and ligament healing and current approaches to tendon and ligament regeneration, J. Orthop. Res. 38 (2020) 7–12, https://doi.org/10.1002/jor.24475.
[2] B.D. Beynnon, R.J. Johnson, J.A. Abate, B.C. Fleming, C.E. Nichols, Treatment of anterior cruciate ligament injuries, Part I, Am. J. Sports Med. 33 (2005) 1579–1602, https://doi.org/10.1177/0363546505279913.
[3] F. Alshomer, C. Chaves, D.M. Kalaskar, Advances in tendon and ligament tissue engineering: materials perspective, J. Mater. 2018 (2018) 9868151, https://doi.org/10.1155/2018/9868151.
[4] C. Yu, S. Feng, Y. Li, J. Chen, Application of nondegradable synthetic materials for tendon and ligament injury, Macromol. Biosci. 23 (2023) 2300259, https://doi.org/10.1002/mabi.202300259.
[5] I. Miescher, J. Rieber, T.A. Schweizer, M. Orlietti, A. Tarnutzer, F. Andreoni, G. Meier Buergisser, P. Giovanoli, M. Calcagni, J.G. Snedeker, A.S. Zinkernagel, J. Buschmann, in vitro assessment of bacterial adhesion and biofilm formation on novel bioactive, biodegradable electrospun fiber meshes intended to support tendon rupture repair, ACS Appl. Mater. Interfaces 16 (2024) 6348–6355, https://doi.org/10.1021/acsami.3c15710.
[6] Y. Wu, Y. Zhang, R. Zhang, S. Chen, Preparation and properties of antibacterial polydopamine and nano-hydroxyapatite modified polyethylene terephthalate artificial ligament, Front. Bioeng. Biotechnol. 9 (2021), https://doi.org/10.3389/fbioe.2021.630745.
[7] B. Farasati Far, M.R. Naimi-Jamal, M. Jahanbakhshi, H. Rostamani, M. Karimi, S. Keihankhadiv, Synthesis and characterization of chitosan/collagen/polycaprolactone hydrogel films with enhanced biocompatibility and hydrophilicity for artificial tendon applications, Int. J. Biol. Macromol. 253 (2023) 127448, https://doi.org/10.1016/j.ijbiomac.2023.127448.
[8] S. Legeay, M. Rodier, L. Fillon, S. Faure, N. Clere, Epigallocatechin gallate: a review of its beneficial properties to prevent metabolic syndrome, Nutrients 7 (2015) 5443–5468, https://doi.org/10.3390/nu7075230.
[9] A. Negri, V. Naponelli, F. Rizzi, S. Bettuzzi, Molecular targets of epigallocatechin—gallate (EGCG): a special focus on signal transduction and cancer, Nutrients 10 (2018) 1936, https://doi.org/10.3390/nu10121936.
[10] G. Iviglia, M. Morra, Engineering interfacial environment of epigallocatechin gallate coated titanium for next-generation bioactive dental implant components, Int. J. Mol. Sci. 24 (2023) 2661, https://doi.org/10.3390/ijms24032661.
[11] M. Sandomierski, M. Chojnacka, M. Ratajczak, A. Voelkel, Zeolites with divalent ions as carriers in the delivery of epigallocatechin gallate, ACS Biomater Sci. Eng. 9 (2023) 5322–5331, https://doi.org/10.1021/acsbiomaterials.3c00599.
[12] S. Demirci, Z. Ustaoğlu, G.A. Yılmazer, F. Sahin, N. Baç, Antimicrobial properties of zeolite-x and zeolite-a ion-exchanged with silver, copper, and zinc against a broad range of microorganisms, Appl. Biochem. Biotechnol. 172 (2014) 1652–1662, https://doi.org/10.1007/s12010-013-0647-7.

[13] P. Kushram, U. Majumdar, S. Bose, Hydroxyapatite coated titanium with curcumin and epigallocatechin gallate for orthopedic and dental applications, Biomater. Adv. 155 (2023) 213667, https://doi.org/10.1016/j.bioadv.2023.213667.
[14] Z.H. Chohan, C.T. Supuran, A. Scozzafava, Metal binding and antibacterial activity of ciprofloxacin complexes, J. Enzyme Inhib. Med. Chem. 20 (2005) 303–307, https://doi.org/10.1080/14756360310001624948.
[15] P. Schacht, G. Arcieri, R. Hullmann, Safety of oral ciprofloxacin: an update based on clinical trial results, Am. J. Med. 87 (1989) S98–S102, https://doi.org/10.1016/0002-9343(89)90033-8.
[16] J. Jaworska, K. Jelonek, M. Jaworska-Kik, M. Musiał-Kulik, A. Marcinkowski, J. Szewczenko, W. Kajzer, M. Pastusiak, J. Kasperczyk, Development of antibacterial, ciprofloxacin-eluting biodegradable coatings on Ti6Al7Nb implants to prevent peri-implant infections, J. Biomed. Mater. Res. A 108 (2020) 1006–1015, https://doi.org/10.1002/jbm.a.36877.
[17] Common Buffers, Media, and Stock Solutions, Current Protocols in Human Genetics 26 (2000) A.2D.1-A.2D.13. doi: 10.1002/0471142905.hga02ds26.
[18] M. He, X. Gao, Y. Fan, L. Xie, M. Yang, W. Tian, Tannic acid/Mg2+-based versatile coating to manipulate the osteoimmunomodulation of implants, J. Mater. Chem. B 9 (2021) 1096–1106, https://doi.org/10.1039/D0TB01577F.
[19] M. Alhafez, F. Kheder, M. Aljoubbeh, Synthesis, characterization and antioxidant activity of EGCG complexes with copper and zinc ions, J. Coord. Chem. 72 (2019) 2337–2350, https://doi.org/10.1080/00958972.2019.1638510.
[20] M. Salman, M.S. Refat, S.A. El-Korashy, M.A. Hussien, Synthesis and spectroscopic characterization of Zn(II), Cd(II), and Hg(II) ciprofloxacin complexes, Russ. J. Gen. Chem. 84 (2014) 1841–1846, https://doi.org/10.1134/S1070363214090345.
[21] A. Domke, M. Fischer, M. Jakubowski, A. Pacholak, M. Ratajczak, A. Voelkel, M. Sandomierski, Experimental and computational study on the Ca2+, Mg2+, Zn2+ and Sr2+ exchanged zeolites as a drug delivery system for fluoroquinolone antibiotic – Ciprofloxacin, J. Drug Delivery Sci. Technol. 99 (2024) 105997, https://doi.org/10.1016/j.jddst.2024.105997.
[22] High Resolution XPS of Organic Polymers: The Scienta ESCA300 Database (Beamson, G.; Briggs, D.) | Journal of Chemical Education, (n.d.). https://pubs.acs.org/doi/10.1021/ed070pA25.5 (accessed December 1, 2024).
[23] A.V. Naumkin, A. Kraut-Vass, S.W. Gaarenstroom, C.J. Powell, NIST X-ray Photoelectron Spectroscopy Database Version 5.0, in: n.d. http:/srdata.nist.gov/xps/, 2023.
[24] D. Briggs, Surface Analysis of Polymers by XPS and Static SIMS, Cambridge University Press, 1998.
[25] E. Matijevic, ed., Medical Applications of Colloids, Springer, New York, NY, 2008. doi: 10.1007/978-0-387-76921-9.
[26] J. Wu, S. Jiang, W. Xie, Y. Xue, M. Qiao, X. Yang, X. Zhang, Q. Wan, J. Wang, J. Chen, X. Pei, Surface modification of the Ti surface with nanoscale bio-MOF-1 for improving biocompatibility and osteointegration in vitro and in vivo, J. Mater. Chem. B 10 (2022) 8535–8548, https://doi.org/10.1039/D2TB01311H.
[27] Y. Boulmokh, K. Belguidoum, F. Meddour, H. Amira-Guebailia, Investigation of antioxidant activity of epigallocatechin gallate and epicatechin as compared to resveratrol and ascorbic acid: experimental and theoretical insights, Struct. Chem. 32 (2021) 1907–1923, https://doi.org/10.1007/s11224-021-01763-5.
[28] P. Brouqui, M.C. Rousseau, A. Stein, M. Drancourt, D. Raoult, Treatment of Pseudomonas aeruginosa-infected orthopedic prostheses with ceftazidime-ciprofloxacin antibiotic combination, Antimicrob. Agents Chemother. 39 (1995) 2423–2425, https://doi.org/10.1128/aac.39.11.2423.
[29] A. Przekora, A concise review on tissue engineered artificial skin grafts for chronic wound treatment: can we reconstruct functional skin tissue in vitro? Cells 9 (2020) 1622, https://doi.org/10.3390/cells9071622.
[30] W. Adamus-Białek, M. Wawszczak, M. Arabski, M. Majchrzak, M. Gulba, D. Jarych, P. Parniewski, S. Głuszek, Ciprofloxacin, amoxicillin, and aminoglycosides stimulate genetic and phenotypic changes in uropathogenic Escherichia coli strains, Virulence 10 (2019) 260–276, https://doi.org/10.1080/21505594.2019.1596507.
[31] M. Cerioli, C. Batailler, A. Conrad, S. Roux, T. Perpoint, A. Becker, C. Triffault-Fillit, S. Lustig, M.-H. Fessy, F. Laurent, F. Valour, C. Chidiac, T. Ferry, Pseudomonas aeruginosa Implant-Associated Bone and Joint Infections: Experience in a Regional Reference Center in France, Front. Med. 7 (2020), https://doi.org/10.3389/fmed.2020.513242.
[32] A.S. Othman, I.M. Shamekh, M. Abdalla, W.A. Eltayb, N.A. Ahmed, Molecular modeling study of micro and nanocurcumin with in vitro and in vivo antibacterial validation, Sci. Rep. 13 (2023) 12224, https://doi.org/10.1038/s41598-023-38652-2.
[33] M. Jakubowski, K. Hałas, M. Ratajczak, A. Voelkel, V. Vivcharenko, M. Trzaskowska, A. Przekora, M. Sandomierski, Innovative coating strategies for titanium implants: combining epigallocatechin gallate, zinc ions, and ciprofloxacin to combat infection and promote osseointegration, Appl. Surf. Sci. 700 (2025) 163243, https://doi.org/10.1016/j.apsusc.2025.163243.
[34] J.A. Hoogkamp-Korstanje, In-vitro activities of ciprofloxacin, levofloxacin, lomefloxacin, ofloxacin, pefloxacin, sparfloxacin and trovafloxacin against gram-positive and gram-negative pathogens from respiratory tract infections, J. Antimicrob. Chemother. 40 (1997) 427–431, https://doi.org/10.1093/jac/40.3.427.
[35] V. Talla, P. Veerareddy, Oxidative stress induced by fluoroquinolones on treatment for complicated urinary tract infections in Indian patients, J. Young Pharm. 3 (2011) 304–309, https://doi.org/10.4103/0975-1483.90242.
[36] E. Emri, E. Miko, P. Bai, G. Boros, G. Nagy, D. Rózsa, T. Juhász, C. Hegedűs, I. Horkay, É. Remenyik, G. Emri, Effects of non-toxic zinc exposure on human epidermal keratinocytes†, Metallomics 7 (2015) 499–507, https://doi.org/10.1039/c4mt00287c.
[37] M. Eghbal, M. Rozman, V. Kononenko, M. Hočevar, D. Drobne, A549 cell-covered electrodes as a sensing element for detection of effects of Zn2+ ions in a solution, Nanomaterials 12 (2022) 3493, https://doi.org/10.3390/nano12193493.
[38] A.F. Abdul Latip, M.Z. Hussein, J. Stanslas, C.C. Wong, R. Adnan, Release behavior and toxicity profiles towards A549 cell lines of ciprofloxacin from its layered zinc hydroxide intercalation compound, Chem. Central J. 7 (2013) 119, https://doi.org/10.1186/1752-153X-7-119.
[39] U. Hofmann, M. Priem, C. Bartzsch, T. Winckler, K.-H. Feller, A sensitive sensor cell line for the detection of oxidative stress responses in cultured human keratinocytes, Sensors 14 (2014) 11293–11307, https://doi.org/10.3390/s140711293.